CHEMISTRY OF MATERIALS
Article

Chem. Mater. **2011,** *23,* 9–13 9
DOI:10.1021/cm100808f

Water-Soluble Graphite Nanoplatelets Formed by Oleum Exfoliation of Graphite

Arnab Mukherjee,[†] JungHo Kang,[‡] Oleksandr Kuznetsov,[§] Yanqiu Sun, Ryan Thaner,[†] Ariana S. Bratt,[†] Jay R. Lomeda,[†] Kevin F. Kelly,*[,‡] and W. E. Billups*[,†]

[†]*Department of Chemistry and The Richard E. Smalley Institute for Nanoscale Science and Technology,* [‡]*Department of Electrical and Computer Engineering, and* [§]*Department of Physics and Astronomy, Applied Physics Program, Rice University, Houston, Texas, United States*

Received March 21, 2010. Revised Manuscript Received November 13, 2010

A facile route to water-soluble graphite nanoplatelets that uses graphite as the starting material is described. The method relies on the addition of phenyl radicals with subsequent sulfonation of the phenyl groups. Atomic force microscopy, high-resolution transmission electron microscopy, and scanning tunneling microscopy images show that a high degree of exfoliation occurs during the sulfonation step. The sheet resistance of the bulk films of the nanoplatelets prepared by vacuum filtration using an anodisc membrane was found to be 212 Ω/sq.

Introduction

The desirable mechanical and electrical properties of graphene have led to intense interest recently in the development of efficient, scalable routes to this material. Graphene is a single-atom thick sheet of hexagonally arrayed sp^2-bonded carbon atoms, which has recently been characterized as the thinnest material on earth.[1] Diverse applications in composite materials,[2−5] liquid crystals,[6] electrical circuits,[7] and quantum dots[8,9] can be expected. Efficient exfoliation[10−17] of precursor materials is a major barrier in the synthesis of graphene/graphite nanoplatelets. Exfoliation has been achieved by either peeling the top surface of pyrolytic graphite[10,18] or by exfoliation of the oxidation products of graphite (graphite oxide).[19,20] Various reagents have been used to remove the oxygen functionality from graphite oxide. A recent report describes a two-step route to water-soluble graphene.[21] In this process, graphite oxide was prepared by oxidizing graphite with acid. The oxygen was then partially removed and *p*-phenyl-SO_3H groups were introduced by diazotization using the benzene diazonium salt of sulfamic acid. Hydrazine was then used to remove the remainder of the oxygen. In this manuscript, we describe a facile route to water-soluble graphite nanoplatelets that uses defect free graphite as the initial point of departure. The method finds analogy in our earlier work on the synthesis of water-soluble carbon nanotubes.[22]

Experimental Section

Commercially available synthetic graphite powder (Sigma Aldrich, particle size less than 20 μm) was used for this study. X-ray photo electron spectroscopy (XPS) analysis of the pure graphite reveals the presence of mainly carbon (96.2%) and

*To whom correspondence should be addressed. E-mail: kkelly@rice.edu (K.F.K.), billups@rice.edu (W.E.B.). Phone: 713 348 3565 (K.F.K.), 713 348 5694 (W.E.B.).

(1) Geim, A. K.; MacDonald, A. H. *Phys. Today* **2007**, *60*, 35–41.
(2) Stankovich, S.; Dikin, D. A.; Dommett, G. H. B.; Kohlhaas, K. M.; Zimney, E. J.; Stach, E. A.; Piner, R.; Nguyen, S. T.; Ruoff, R. S. *Nature* **2006**, *442*, 282–286.
(3) Stankovich, S.; Dikin, D. A.; Piner, R.; Kohlhaas, K. M.; Kleinhammes, A.; Jia, Y.; Wu, Y.; Nguyen, S. T.; Ruoff, R. S. *Carbon* **2007**, *45*, 1558–1565.
(4) Ramanathan, T.; Abdala, A. A.; Stankovich, S.; Dikin, D. A.; Herrera-Alonso, M.; Piner, R. D.; Adamson, D. H.; Schniepp, H. C.; Chen, X.; Ruoff, R. S.; Nguyen, S. T.; Aksay., I. A.; Prud'homme, R. K.; Brinson, L. C. *Nature* **2008**, *3*, 327–331.
(5) Watchartone, S.; Dikin, D. A.; Stankovich, S.; Piner, R.; Jung, I.; Dommett, G. H. B.; Evmeneko, G.; Wu, S. E.; Chen, S. F.; Liu, C. P.; Nguyen, S. T.; Ruoff, R. S. *Nano Lett.* **2007**, *7*, 1888–1892.
(6) Blake, P.; Brimicombe, P. D.; Nair, R. R.; Booth, T. J.; Da, J.; Schedin, F.; Ponomarenko, L. A.; Morozov, S. V.; Gleeson, H. F.; Hill, E. W.; Geim, A. K.; Novosolev, K. S. *Nano Lett.* **2008**, *8*, 1704–1708.
(7) Hong, S.; Yoon, Y.; Guo, J. *Appl. Phys. Lett.* **2008**, *92*, 083107–083109.
(8) Zhang, Y.; Tan, Y.-W.; Stromer, H. L.; Kim., P. *Nature* **2005**, *438*, 201–204.
(9) Pereira, J. M.; Vasilopoulos, P.; Peeters, F. M. *Nano Lett.* **2007**, *7*, 946–949.
(10) Geim, A. K.; Novosoelov, K. S. *Nat. Mater.* **2007**, *6*, 183–191.
(11) Wu, J.; Pisula, W.; Mullen, K. *Chem. Rev.* **2007**, *107*, 718–747.
(12) Novosoelov, K. S.; Geim, A. K.; Morozov, S. V.; Jiang, D.; Zhang, Y.; Dubonos, S. V.; Grigorieva, I. V.; Firsov, A. A. *Science* **2004**, *306*, 666–669.
(13) Novosoelov, K. S.; Geim, A. K.; Morozov, S. V.; Jiang, D.; Katsnelson, M. I.; Dubonos, S. V.; Firsov, A. A. *Nature* **2005**, *438*, 197–200.
(14) Zheng, W.; Wong, S. C. *Compos. Sci. Technol.* **2003**, *63*, 225–235.
(15) Novosoelov, K. S.; Jiang, Z.; Zhang, Y.; Morozov, S. V.; Stromer, H. L.; Zeitler, U.; Maan, J. C.; Boebinger, G. S.; Kim, P.; Geim, A. K. *Science* **2007**, *315*, 1379–1379.
(16) Brink, J. V. D. *Nat. Nanotechnol.* **2007**, *2*, 199–201.
(17) White, C. T.; Li, J.; Gunlycke, D.; Mintmire, J. W. H. *Nano Lett.* **2007**, *7*, 825–830.
(18) Ponomarenko, L. A.; Schedin, F.; Katsnelson, M. I.; Yang, R.; Hill, E. W.; Novoselov, K. S.; Geim, A. K. *Science* **2008**, *320*, 356–358.
(19) Gilje, S.; Han, S.; Wang, M.; Kang, K. L.; Kaner, R. B. *Nano Lett.* **2007**, *7*, 3394–3398.
(20) Gómez-Navarro, C.; Weitz, R. T.; Bittner, A. M.; Scolari, M.; Mews, A.; Burghard, M.; Kern, K. *Nano Lett.* **2007**, *7*, 3499–3503.
(21) Si, Y.; Samulski, E. T. *Nano Lett.* **2008**, *8*, 1679–1682.
(22) Liang, F.; Beach, J. M.; Rai, P. K.; Guo, W. H.; Hauge, R. H.; Pasquali, M.; Smalley, R. E.; Billups, W. E. *Chem. Mater.* **2006**, *18*, 1520–1524.

Published on Web 12/10/2010

Scheme 1. Synthesis of Water-Soluble Graphite Nanoplatelets

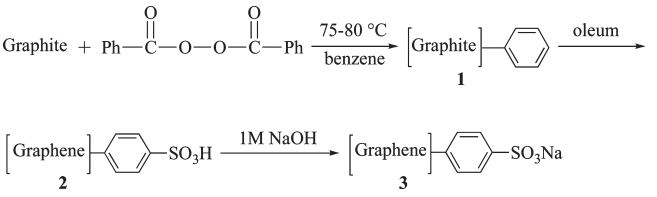

oxygen (~3%). The dark gray graphite powder (50 mg, 4.16 mmol of carbon) was dispersed in benzene (70 mL) in a 100 mL three-necked round-bottom flask equipped with a magnectic stir bar. The contents were then stirred vigorously as benzoyl peroxide (1.01 g, 4.16 mmol) was added. The mixture was then heated under argon at 80 °C for 2 h with continuous vigorous stirring. After cooling, the contents of the flask were diluted with benzene (100 mL), filtered through a PTFE membrane (0.2 μm), and washed with chloroform. The phenylated graphite **1** (20 mg) was then dispersed in oleum (20 mL, H_2SO_4, 20% as free SO_3), and heated under argon at 80 °C for 4 h to yield phenyl sulfonated **2**. The suspension was then poured carefully into 100 mL of ice water, filtered through a polycarbonate membrane (0.22 μm), and washed with water. The phenyl sulfonated salt **3** was prepared by heating a dispersion of **2** (20 mg) in 1 M NaOH (30 mL) overnight at 80 °C under argon (Scheme 1). The contents were then diluted by water (100 mL), filtered through a polycarbonate membrane (0.22 μm), and washed carefully with water.

Characterization. The products were characterized by Raman spectroscopy, FT-IR spectroscopy with ATR accessory, thermogravimatric analysis (TGA), XPS, atomic force microscopy (AFM), high-resolution transmission electron microscopy (HRTEM), and scanning tunneling microscopy (STM). All characterizations were performed on powders. Raman spectra were collected from samples, using a Renishaw 1000 micro-Raman system with a 514 nm laser source. Multiple spectra (3−5) were obtained, normalized to the G band, and averaged to present a comprehensive snapshot of the material. FTIR spectra were obtained using a Nicolet spectrometer with the ATR accessory. TGA data were obtained using a model SDT 2960 TA Instruments in argon atmosphere. Samples were degassed at 80 °C and then heated at 10 °C/min to 700 °C and held there for 20 min. XPS data were obtained using a physical electronics (PHI QUANTERA) XPS/ESCA system. The base pressure was at 5×10^{-9} Torr. A monochromatic Al X-ray source at 100 W was used with pass energy of 26 eV and with a 45° takeoff angle. The beam diameter was 100.0 μm. Low-resolution survey scans and higher resolution scans of C, O, and S were taken. At least two separate locations were analyzed for each sample. AFM was performed using a Digital Instruments Nanoscope IIIa in tapping mode using a 3045 JVW piezo tube scanner. A scan frequency of 1.0 Hz was used. HRTEM images are taken using a high-resolution transmission electron microscope (HRTEM, JEM-2010F) operated at an accelerating voltage of 200 kV. STM was performed by drop casting the graphitic nanoparticles onto Au(111) on mica and subsequently scanned using a variable-temperature ultrahigh vacuum Omicron system controlled by RHK Technology electronics.

Results and Discussion

Water-soluble graphite nanoplatelets **2** and **3** can be prepared as illustrated in Scheme 1, a route similar to that demonstrated earlier for carbon nanotubes[22] where highly

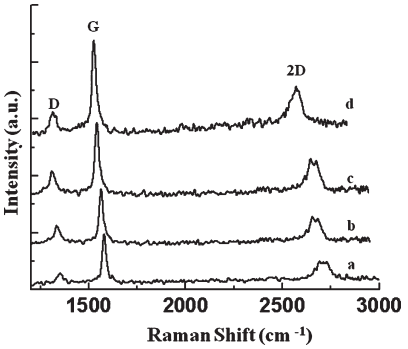

Figure 1. Raman spectra of (**a**) graphite (**b**) phenylated graphite **1** (**c**) sulfonated graphite nanoplatelets **2** (**d**) sodium salt **3** of sulfonated graphite nanoplatelets **2**.

cohesive van der Waals attractions[23] were overcome by sulfonation in oleum. Thus, addition of benzoyl peroxide to a suspension of graphite in benzene at 75−80 °C provides the phenylated graphite **1**. Sulfonation of **1** by oleum leads to the highly exfoliated graphite nanoplatelets **2**. The salt **3** was prepared by adding 1 M sodium hydroxide to **2**. This material was found to exhibit high solubility in water (2.1 mg/mL). As the following analysis will show, the functionalized product **3** is not only highly soluble thanks to the attachment of the sodium sulfonate groups, but it is also relatively free of the basal plane defects that typically result from removal of the oxygen functionality of comparable graphite oxide (GO) compounds.

An XPS study of **2** confirmed the presence of sulfur (S $2p_{3/2}$ and S $2p_{1/2}$) with peaks at ~168 eV. The sodium salt **3** shows peaks corresponding to both sodium and sulfur (Supporting Information, Figure 1). The attenuated total reflectance (ATR) Fourier transform infrared (FTIR) spectrum shows a broad hump at ~1200 cm^{-1} that confirms the presence of the sulfonic acid group (ν_{S-O} and $\nu_{S\text{-phenyl}}$).[21] Peaks at ~950 (ν_{C-H} in-plane bending) and 830 cm^{-1} (out-of-plane hydrogen wagging) represent characteristic vibrations of a *p*-disubstituted phenyl group.[32] Once successful functionalization was confirmed, the next step was evaluating the extent of changes to the structure of the graphitic layers.

The Raman spectra of **1**−**3** are presented in Figure 1. The *D*, *G* and 2*D* bands were recorded using 514.5 nm laser excitations. The starting graphite powder (Figure 1a) exhibits weak *D* and 2*D* bands that arise from defects. Functionalization of the graphitic edges might account for the weak enhancement of the *D* band. According to previous studies,[24,25] the electronic structure of graphene is captured in its Raman spectra, and the graphene layers can be identified by monitoring the position of the 2*D* band. Sulfonation of the phenyl groups and the resulting repulsive interaction between the $—SO_3^{\delta-}$ groups leads to partial exfoliation as observed by the downshift of the 2*D* peak. Finally, when the sodium salt is formed, a high degree of exfoliation (corresponding to ~5 layers of graphene) is observed as demonstrated by the sharp 2*D*

(23) Zacharia, R.; Ulbricht, H.; Hertel, T. *Phys. Rev. B* **2004**, *69*, 155406–155407.

(24) Ferrari, A. C. *Solid State Commun.* **2007**, *143*, 47–57.

(25) Ferrari, A. C.; Meyer, J. C.; Scardaci, V.; Casiraghi, C.; Lazzeri, M.; Mauri, F.; Piscanec, S.; Jiang, D.; Novoselov, K. S.; Roth, S.; Geim, A. K. *Phys. Rev. Lett.* **2006**, *97*, 187401–187404.

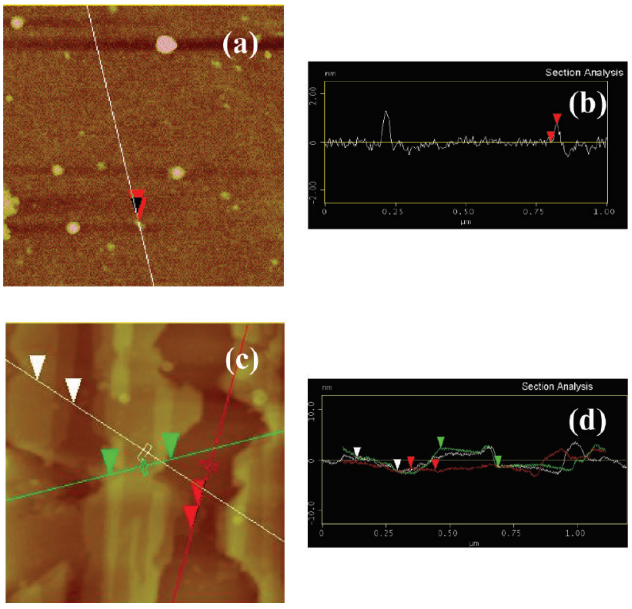

Figure 2. (**a**) Tapping mode AFM amplitude image ($5 \times 5\,\mu m^2$) of graphene **2** spin coated onto freshly cleaved mica from water. (**b**) AFM section analysis of **2**. *x* axis in μm and *y* axis in nm. (**c**) AFM amplitude image ($1 \times 1\,\mu m^2$) of **3** spin coated onto freshly cleaved mica from water. (**d**) AFM section analysis of **3**. *x* axis in μm and *y* axis in nm. The colored triangles indicate the section analysis for different points of functionalized graphene.

peak which is shifted by $\sim$100 cm^{-1} relatively to the same peak in the starting material. This is attributed to charge repulsion of the SO_3^- groups[24,25]

Detachment of the functional groups from **2** during thermogravimetric analysis (TGA) leads to a weight loss of 18%, indicating that one functional group is present for approximately 50 graphitic carbon atoms. This level of functionalization is consistent with the enhancement of the *D* band (Figure 1) and emphasizes the efficiency of the functionalization process.

To characterize the exfoliated product by AFM, a solution (0.2 mg/mL) of **3** in water was spin coated onto mica. As shown in Figure 2a, the solution consisted mostly of irregular, graphitic nanoplatelets.[26] Height analysis in Figure 2b shows sheets with heights from $\sim$0.6 nm to $\sim$5 nm. A bare graphene sheet is less than 1 nm[20,27,28] whereas the theoretical height of graphene sheets functionalized on both sides is expected to be somewhat thicker.[29] The overall accuracy of this measurement is limited in its *z*-resolution. A more precise observation via tunneling micrscopy is discussed below. Some of the sheets in Figure 2c appear to be folded along the edges. This phenomenon is observed frequently in tapping mode AFM images of graphene.[30]

Figure 3 shows the high-resolution TEM images of synthetic graphite and the sodium salt **3**. The graphite shows a large number of graphene sheets stacked as shown in Figure 3a. The high resolution TEM image of the graphene functionalized by sulphonated phenyl groups in Figure 3b shows about five layers of stacked graphene sheets.[31] All of these experiments suggest the formation of exfoliated graphene sheets varying from single to $\sim$10 layers similar to that obtained by other chemical methods.[21]

To examine the atomic-scale structure, exfoliated graphene sheets of **3** were deposited onto Au(111) substrates and imaged by a scanning tunneling microscope (STM). The height of the graphitic nanostructures ranged from less than 2 and up to 5 nm, which corresponds to between 5 and 14 layers. Figures 4a and 4b correspond to topographs from two such nanoparticles. Cross sections through each of these are displayed in Figure 4c, allowing the extrapolation of the number of layers. A high-pass filtered image of Figure 4b in 4d reveals the individual domains of the different layers.

Figure 4b contains an exfoliated single layer of graphene in the lower left portion of the image attached to the adjacent larger structure. Upon close inspection, clear atomic resolution was observed in several of the exfoliated sheets, one of which is shown in Figure 5a. Even at this scale, any defects on the terraces would be readily apparent in the STM images.[35] The corresponding height cross-section displayed in Figure 5b shows clear quantized steps between these terraces that correspond well with expected interlayer spacing of bulk graphite. Figure 5c is a high-resolution image of the pristine atomic structure. Figure 5d is the corresponding 2D Fourier transform of this image that further confirms the graphitic atomic structure. This strongly supports the previous conclusion that the functionalization is performed on the dangling bonds at the edges without perturbing the sp^2 bonds of the basal plane.[31] It also explains the weak *D* band appearance in the Raman spectra. The comparison of rms edge roughness measurement of the exfoliated graphite **3** to that of highly ordered bulk pyrolytic graphite shows higher roughness for the exfoliated graphite because of the functional groups on the edge. We have quantified the roughness of step edges on these samples by comparing it to the roughness of naturally occurring step edges. Because the roughness can vary with bias conditions, scan size, and scan resolution, we have chosen to quantify relative roughness by comparing the roughness of the upper terrace step edges in these two systems directly to adjacent areas on the terrace of equal size. We have found that the roughness of naturally occurring step edges reveal an rms roughness $\sim$20% greater than the adjacent bare terrace region. On the other hand, the step edges of the functionalized graphitic nanoparticles reveal a

(26) Schniepp, H. C.; Li, J.; McAllister, M. J.; Sai, H.; Herrera-Alonso, M.; Adamson, D. H.; Prud'homme, R. K.; Car, R.; Saville, D. A.; Aksay, I. A. *J. Phys. Chem. B* **2006**, *110*, 8535–8539.
(27) Stankovich, S.; Piner, R. D.; Chen, X. Q.; Wu, N. Q.; Nguyen, S. T.; Ruoff, R. S. *J. Mater. Chem.* **2006**, *16*, 155–158.
(28) Becerril, H. A.; Mao, J.; Liu, Z.; Stoltenberg, R. M.; Bao, Z.; Chen, Y. *ACS Nano* **2008**, *2*, 463–470.
(29) Lomeda, J. R.; Doyle, C. D.; Kosynkin, D. V.; Hwang, W.-F.; Tour, J. M. *J. Am. Chem. Soc.* **2008**, *130*, 16201–16206.
(30) Nemes-Incze, P.; Osváth, Z.; Kamarás, K.; Biró, L. P. *Carbon* **2008**, *46*, 1435–1442.
(31) Chattopadhyay, J.; Mukherjee, A.; Hamilton, C.; Kang, J. H.; Chakraborty, S.; Guo, W. H.; Kelly, K. F.; Barron, A. R.; Billups, W. E. *J. Am. Chem. Soc.* **2008**, *130*, 5414–5415.
(32) Colthup, N. B.; Daly, L. H.; Wiberley, S. E. *Introduction to Infrared and Raman Spectroscopy*, 3rd ed.; Academic Press: London, 1990.
(33) Wang, X.; Zhi, L.; Mullen, K. *Nano Lett.* **2008**, *8*, 323–327.
(34) Kim, K. S.; Zhao, Y.; Jang, H.; Lee, S. Y.; Kim, J. M.; Kim, K. S.; Ahn, J.-H.; Kim, P.; Choi, J.-Y.; Hong, B. H. *Nature* **2009**, *457*, 706–710.
(35) Kelly, K. F.; Mickelson, E. T.; Hauge, R. H.; Margrave, J. L.; Halas, N. J. *Proc. Natl. Acad. Sci. U.S.A.* **2000**, 10318–10321.

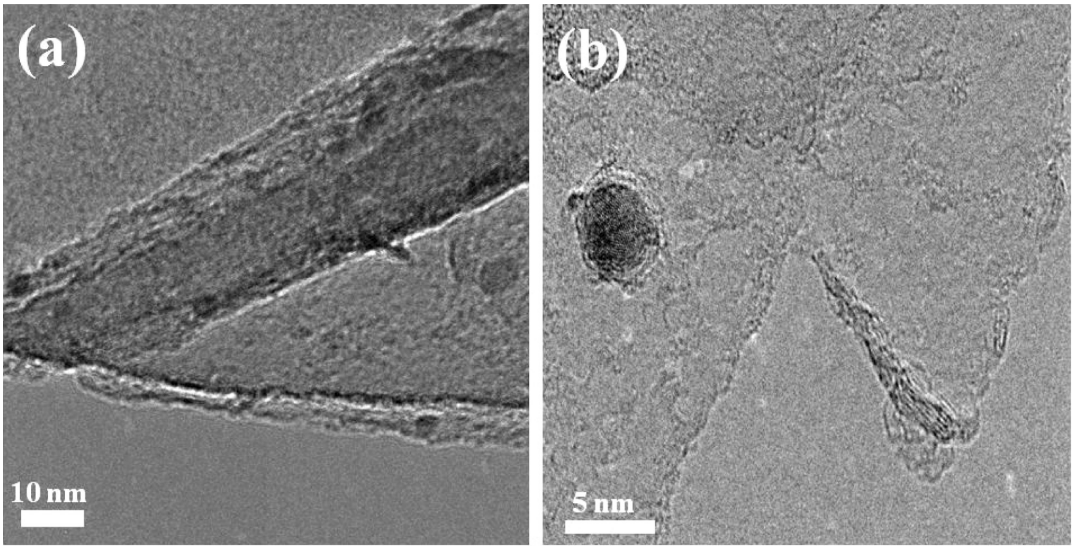

Figure 3. (**a**) HRTEM image of synthetic graphite. (**b**) HRTEM image of graphene **3**.

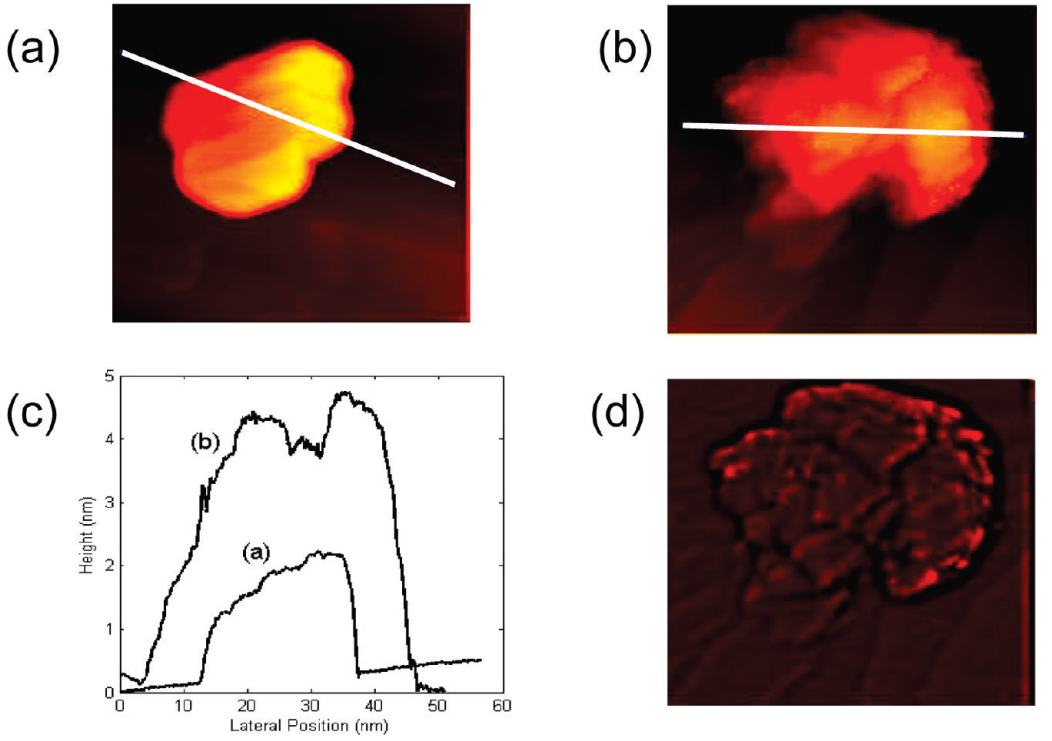

Figure 4. (**a**), (**b**) STM images of exfoliated graphene on Au(111) substrates. (**a**) Image size: (57.6 × 57.6 nm2), bias voltage [V_{bias}] = 100 mV, tunneling current [I_t] = 0.1 nA, (**b**) (56 × 56 nm2), [V_{bias}] = −200 mV, [I_t] = 1 nA. (**c**) Cross sections of (**a**) and (**b**). (**d**) A high-pass filtered image of (**b**) showing different domains and a single layer attached to multiple-layered structure.

consistent roughness ~60% greater than the adjacent terrace. This result coupled with an absence of defects on the terrace as seen by imaging the unperturbed lattice, strongly suggests that the chemical modification has occurred only at the edges of these nanoparticles.

Stable solutions of **3** in water are formed after sonication for a few minutes (Figure 6). These solutions remain stable indefinitely.

The sheet resistance of bulk films prepared by vacuum filtration using an anodisc membrane (pore size ~20 nm) was determined using a four-point probe fitted to a custom built attachment with Pt leads for film testing. Graphene **2** gave an average value of 212 Ω/sq, while the starting graphite gave 960 Ω/sq. Thin film samples prepared from graphene oxide give a sheet resistance of about 1.8 kΩ/sq after annealing.[34] These measurements support our belief that chemical functionalization under these conditions preserves the crystalline structure of the graphene basal planes. Materials prepared from our water-soluble material will likely result in much higher conductivity than previous methods. For comparion, the value reported for graphene grown on Ni by Kim et al. is ~280 Ω/sq.[34] We suspect that ionic conduction may play a role in the high conductivity that we observe. A similar

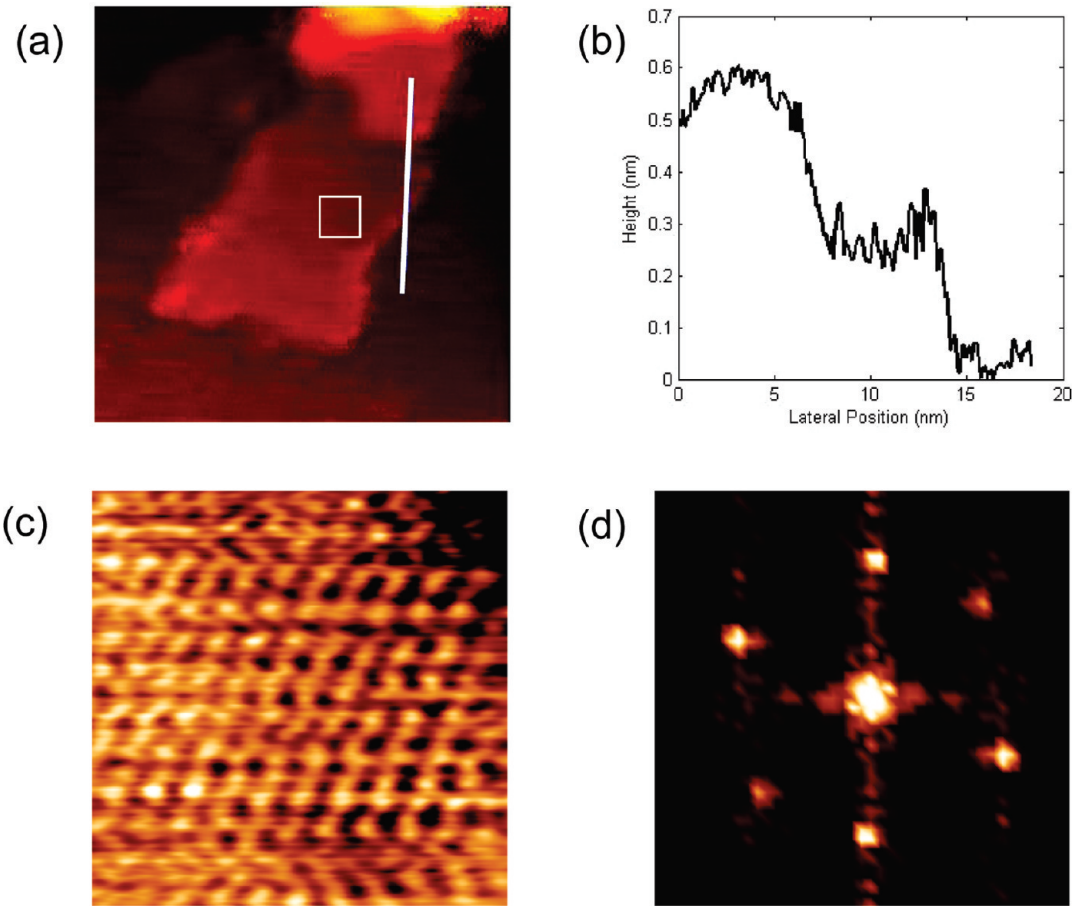

Figure 5. (**a**) Single layer of exfoliated graphene from lower left of Figure 4(b) showing defects on the edges. Imaging condition: (33.7 × 33.7 nm2), [V_{bias}] = −83 mV, [I_t] = 1.5 nA. (**b**) Cross-section of (**a**) showing normal layer spacing of graphite. (**c**) Atomic structure from the boxed area of (**a**). Imaging condition: (3.6 × 3.6 nm^2), [V_{bias}] = −83 mV, [I_t] = 2.3 nA. (**d**) 2D Fourier transform of (**c**).

Figure 6. Aqueous solution of **3**.

interpretation has been presented for carbon nanotubes that were functionalized using the same protocol.[36]

(36) Glover, B.; Whites, K.; Hong, H.; Mukerjee, A.; Billups, W. E. *Synth. Met.* **2008**, *158*, 506.

Conclusions

An efficient route to highly exfoliated water-soluble graphite nanoparticles that uses non-oxidized graphite as a starting material is described. The final exfoliated material shows pristine atomic structure on the basal plane with functional groups only along the edges. The material has an average sheet resistance that is lower than the starting graphite. It remains suspended in water indefinitely and exists in the form of single to a few layers of graphene as determined by microscopy studies.

Acknowledgment. This work was supported in part by the Robert A. Welch Foundation (C-0490 and C-1605), the National Science Foundation (CHE-0450085), and the Houston Area Research Council.

Supporting Information Available: XPS data and ATR-FTIR spectra of unfunctionalized and phenyl sulfonated graphite. This material is available free of charge via the Internet at http://pubs.acs.org.